Original Article

# Assessment of Manganese-Zinc Ferrite Nanoparticles as a Novel Magnetic Resonance Imaging Contrast Agent for the Detection of 4T1 Breast Cancer Cells

**Tayebe Sobhani[1], Daryoush Shahbazi-Gahrouei[1], Mahboubeh Rostami[2], Maryam Zahraei[3], Amin Farzadniya[4]**

*[1]Department of Medical Physics, School of Medicine, Isfahan University of Medical Sciences, [2]Department of Medicinal Chemistry, School of Pharmacy and Pharmaceutical Sciences, Isfahan University of Medical Sciences, [3]Department of Materials Engineering, Isfahan University of Technology, [4]Department of Radiology, Askarieh Hospital, Isfahan, Iran*

## Abstract

**Background:** The aim of the study was to evaluate the potential of manganese-zinc ferrite nanoparticles (MZF NPs) as a novel negative magnetic resonance imaging (MRI) contrast agents for 4T1 (mouse mammary carcinoma) and L929 (murine fibroblast) cell lines. **Methods:** MZF NPs and its suitable coating, polyethylene glycol (PEG) via covalent bonding, were investigated under *in vitro* condition. The cytotoxicity of MZF NPs was tested by 3-(4,5-dimethyl thiazolyl-2)-2,5-diphenyltetrazolium bromide assay after 12 and 24 h of incubation. To evaluate the potential of MZF NPs as $T_2$ MRI nanocontrast agent, images were obtained from phantom containing different Fe concentrations and $T_2$ relaxivity ($r_2$) was measured. The viability of both 4T1 breast cancer and L929 murine fibroblast cell lines incubated with different Fe concentrations. **Results:** *In vitro* $T_2$-weighted MRI showed that signal intensity of 4T1 cells was lower than that of L929 as control cells. $T_2$-weighted MRI showed that signal intensity of MZF NPs enhanced with increasing concentration of NPs. The values of $1/T_2$ relaxivity ($r_2$) for coated MZF NPs with PEG found to be 85.5 $mM^{-1}$ $s^{-1}$ which is higher than that of commercially clinical used (Sinerem) MRI contrast agent. **Conclusion:** The results showed that MZF NPs have potential to detect breast cancer cells (4T1) and also have high contrast resolution between normal (L929) and cancerous cells (4T1) which is a suitable nanoprobe for $T_2$-weighted MR imaging contrast agents.

**Keywords:** *4t1 and l929 cells, contrast agents, magnetic resonance imaging, manganese-zinc ferrite nanoparticles*

**Submitted:** 05-Dec-18 **Revision:** 05-Mar-19 **Accepted:** 19-Mar-19 **Published:** 24-Oct-19

## Introduction

Magnetic resonance imaging (MRI) is one of the most powerful imaging techniques for cancer diagnosis in medicine due to its excellent temporal and spatial resolution (25°–100° μm) and noninvasive imaging modality.[1-3] However, its low sensitivity and unclear diagnosis of healthy tissues from abnormal tissues are a challenge in MRI which is caused by normal and abnormal tissue relaxation time similarity.[4] Therefore, it is necessary to provide excellent sensitivity using MRI contrast agent.

Commonly, MRI contrast agent is gadolinium (Gd) paramagnetic complex diethylenetriaminepentaacetic acid (Gd-DTPA). Gd ions quickly leave the circulatory system and provide a short time for imaging.[1] Furthermore, according to the Food and Drug Administration warning, patients with acute liver and kidney failure who are using Gd-DTPA are at the risk of developing a potentially fatal and nephrogenic systemic fibrosis disease.[5]

During the last decade, ultrasensitive contrast agents, based on superparamagnetic ferrite NPs, have drawn a lot of attention for diagnosis and treatment of cancers due to their higher magnetization and lower concentration employed as compared to common paramagnetic contrast agent.[6] Magnetic nanoparticles (MNPs) can alter longitudinal ($T_1$) and transverse ($T_2$) relaxation times and resulted in changes in MR signal intensity.[7,8]

Comparison of various ferrite NPs has shown that manganese ferrite and especially zinc-substituted manganese



**How to cite this article:** Sobhani T, Shahbazi-Gahrouei D, Rostami M, Zahraei M, Farzadniya A. Assessment of manganese-zinc ferrite nanoparticles as a novel magnetic resonance imaging contrast agent for the detection of 4T1 breast cancer cells. J Med Sign Sens 2019;9:245-51.

***Address for correspondence:***
*Prof. Daryoush Shahbazi-Gahrouei, Department of Medical Physics, School of Medicine, Isfahan University of Medical Sciences, Isfahan, Iran.*
*E-mail: shahbazi@med.mui.ac.ir*

**Access this article online**

**Website:** www.jmssjournal.net

**DOI:** 10.4103/jmss.JMSS_59_18

**Quick Response Code:**

ferrite NPs are great candidates for MRI contrast agents due to higher magnetic susceptibility and magnetic saturation than magnetite and other ferrite NPs.[7,9] According to the literature, application of manganese-zinc ferrite MNPs (MZF NPs) as potential magnetic carriers was conducted by many researchers.[6-10] MZF NPs hydrothermally have been synthesized by Zahraei *et al*. in previous work.[10] To protect the NP from fast blood elimination which is a major challenge in biomedical applications, NPs were modified by polyethylene glycol (PEG) coating.[11-13]

To the best of our knowledge, there is no report on the MRI contrast enhancement effect of MZF NPs in 4T1 and L929 cell lines under *in vitro* conditions. Herein, the investigation of contrast properties of MZF NPs as an MRI contrast agents was introduced, and its cytotoxicity was tested in 4T1 and L929 cell lines by 3-(4,5-dimethyl thiazolyl-2)-2,5-diphenyltetrazolium bromide (MTT) colorimetric assay. To evaluate the potential of MZF NPs as $T_2$ MRI contrast agent, $T_2$-weighted MRI was obtained in phantom containing different concentrations, followed by the measurements of their relaxation rate ($1/T_2$) and relaxivity ($r_2$).

## Materials and Methods

### Nanoparticles synthesis and surface modification

The synthesis and purification of MZF NPs were done based on a previously published procedure.[10] Briefly, MZF NPs with size of 14 nm were obtained via the hydrothermal method. To improve their size, monodispersity, and crystallinity and activate their surface, the sample was subjected to an acid treatment.[14] Finally, PEG (PEG-NH2 [methoxy-PEG amine]) with a molecular weight of 20 kDa was covalently anchored to carboxyl groups of the NPs surface through their amine group via EDC (1-ethyl-3-(3-dimethylaminopropyl)-carbodiimide) chemistry.[10]

### Characterization

Colloidal properties, hydrodynamic particle size, and width of the particle size distribution (polydispersity index [PDI]) of NPs were characterized by dynamic light scattering using a Malvern Instrument Zetasizer (DTS version 5.02) provided with a He/Ne laser of 633 nm wavelength.[15] The mean nanoparticles' size was obtained by transmission electron microscope (TEM) using a 200 keV (JOEL 2000 FXII model) electron microscopy.

Elemental analysis was used to quantify Fe in the final composition of the ferrites. The known volumes of MZF NPs suspension were taken in a glass test tube. Samples were dissolved in 12.5 M hydrochloric acid and 5 M nitric acid with a ratio of 3:1 and then stead in an ultrasonic bath (Wiseclean, Korea) at 60°C for 2 h. The iron concentration of samples was measured with the emission of ferrite ions (239.563 nm) by inductively coupled plasma optical emission spectroscopy (Varian vista-pro, Victoria, Australia).

### Cell culture

Mouse mammary carcinoma (4T1) and murine fibroblast (L929) cell lines were purchased from Pasteur Institute (Tehran, Iran). Cells were cultured in RPMI-1640 (Sigma, USA) medium supplemented with 10% fetal bovine serum (FBS) and 1% antibiotic mixture containing penicillin and streptomycin. The cells were incubated at 37°C in a humidified incubator at 5% $CO_2$ atmosphere, and then, they were harvested by trypsin and counted by hemacytometer. All mentioned substances were purchased from Sigma-Aldrich (CA, USA).

### Cytotoxicity assay

To investigate changes in the shape and division of the cells in the effect of MNPs, $10^4$ of 4T1 and L929 cells were incubated with 0.4 mg Fe/ml of MNPs. The control group was without MNPs. After 2 and 24 h, morphology and division of the cells were investigated using the microscope light (Nikon Eclipse TS100 Microscope, Tokyo, Japan).

*In vitro* quantitative cytotoxicity of MNPs was calculated on two different cell lines 4T1 as cancer cell and L929 as a normal cell by MTT colorimetric assay. A number of $10^4$ cells were seeded in 96-well plates (SPL life Science Co., Korea) with 100 µl RPMI-1640/well rich of 10% FBS and 1% antibiotics for 24 h in a humidified incubator because of cell attachment. Then, the medium was removed and replaced with fresh media containing different concentrations of Fe 0, 0.1, 0.2, 0.3, 0.4, 0.5, 0.6, and 0.8 (mg Fe/ml) in nine wells for each Fe concentration for 12 and 24 h. Untreated wells (without MNPs) were used as control group. After the time point, the medium of wells was removed and the wells washed three times with phosphate bovine serum (PBS), following by adding 20 µl of MTT reagent 5 mg/ml in PBS, and 90 µl medium into each well and incubated for 4 h. Afterward, the medium was evicted and 100 µl dimethyl sulfoxide was added to each well for dissolving diphenyltetrazolium crystal. Rate of generation color and absorbance of each well which has a linear relationship with cell survival were measured by a Microplate Reader (Bio-Rad Laboratories, Model 680, Inc., and Hercules, USA) at 570 nm. Cell viability percentage was determined by the following equation:[16]

Cell viability percentage = 100 × (mean absorbance in test wells/mean absorbance in control wells)

### *In vitro* magnetic resonance imaging

$10^6$ cells per well were cultured in six-well plates (SPL life Science Co., Korea) with the 2 ml medium at the humidified incubator for 24 h. Then, the cells were incubated with media containing different concentrations of MNPs (0, 0.1, 0.2, 0.4, 0.6, and 0.8 mg Fe/ml) in a shaker incubator (GFL 3033, MKS) at room temperature. After

4 h, they washed three times with PBS. The cells were suspended in 0.5 ml of low melting temperature with 2% agarose solution. For this purpose, 1 g agarose powder was dissolved in 50 ml water and heated to 50°C with a magnetic stirrer (RH basic 2, IKA, Germany) posterior staid in a bath sonicator (Wiseclean, Wised) for 10 min to obtain uniform solution. The tubes containing cells were quickly homogenized by vortex (IKA Vortex, GENIUS3), placed in a microtube rack (Maxwell, China) underneath ice prouder, and then cooled to 4°C in the icebox for consolidation. The control group was contained $10^6$ cells that suspended in 0.5 ml jelly in the same conditions.

MRI was carried out with MRI scanner (AERA, 1.5 Tesla, 16 channels Siemens Medical system) equipped with head coil at room temperature. $T_2$-weighted axial section images were obtained by multi spin-echo pulse sequence ($T_E$ = 66 ms, $T_R$ = 3000 ms, slice thickness = 3 mm, matrix size = 512 × 364, field of view (FOV) = 22 cm × 22 cm).

### Image processing and analysis

After provision of MRI, for investigating the changing of signal intensity in 2 type cells, an image analysis package (ImageJ 1.51j8 NIH, USA) was used. The average signal intensity was measured by drawing region of interest (ROI) at the identical position of MRI. The signal intensity was consistently gray-scale of ROI in MRI.

The contrast changing between normal and cancer cells was expressed as the enhancement by use of the following equation:

$$\text{Enhancement} = 100 \times SI_{before} - SI_{after}/SI_{before}$$

Where $SI_{before}$ is the signal intensity of cells without MNPs and $SI_{after}$ is the signal intensity of cells with the different concentration of MNPs.

### Relaxivity ($r_2$) measurement

Dispersed MNP in water was suspended in a premade gelatin (2 agarose gel solution as described in the previous section at *in vitro* MRI) to obtain final Fe concentrations and 500 μL final volume. Immediately, the tubes were placed in a 0.5 ml microtube rack (Maxwell, China) in which the icing powder was firmly fixed until they were placed in the refrigerator for imaging. The control group contained 500 μl of gelatin.

The MRI of tubes containing different concentrations of NPs was achieved by the mentioned MRI scanner located at the MRI center of Askarieh Hospital, Isfahan, Iran.

All measurements were carried out at room temperature using multiple spin-echo sequence 16, echo time $T_E$ = 22–352 ms, repetition time $T_R$ = 3000 ms, slice thickness = 3 mm, number of excitation (NEX) = 1, and imaging matrix = 364 × 512.

To obtain $T_2$, a multi-point method was used to determine the signal intensity curve of a 16-echo spin sequence in $T_E$. The signal intensity in a spin-echo sequence protocol is obtained using the following equation:

$$S = S_0 e - T_E/T_2$$

Where $S$ is the signal intensity after administration of different concentration MNPs and $S_0$ is the signal intensity of 500 μl of gelatin.

The spin-spin relaxivity ($r_2$) was calculated by linear curve fitting $1/T_2$ as a function of iron concentration (mM). This calculation was performed using Excel software. After provision of MRI, the average MR signal intensity was determined by drawing the ROIs at the level of each of the samples image with an image analysis package.

### Statistical analysis

All values were represented as mean ± standard deviation. All data were analyzed by two-way analysis of variance (ANOVA) with *post hoc* least significant difference (LSD) tests. Statistical significance was set at $P < 0.05$ ($P < 0.05$, ns: Not significant). Data were collected with Excel software, 2010 and analyzed by SPSS Software version 20.0 (IBM Armonk, NY, USA).

## Results

### Synthesis and characterization of nanoparticles

The surface morphology and size distribution of MZF NPs were evaluated by TEM [Figure 1] and Zetasizer. The findings showed that particles had almost spherical structures. The average particle sizes of synthesized NPs were 14 nm. The hydrodynamic particle size and the PDI of NPs were 392.4 nm and 0.515, respectively.

### Cytotoxicity assay

The morphology of the studied cells incubated with 0.4 mg Fe/ml after 2 and 24 h is shown in Figure 2a and b with phase contrast microscopy. As indicated in this figure, the cells were spread with uniformity shape. Also, 4T1 cells proliferation was lower than that of control cells.

The quantitative effect of the MNPs on 4T1 and L929 cells at 12 and 24 h after incubation with different concentration of MNPs was measured by MTT assay. The control group was no treated cells. The cell viability as a function of concentration of Fe is shown in Figure 3.

As indicated from Figure 3, the viability of L929 at 12 and 24 h for all concentrations was higher than 80%, which shows that the NPs have no toxicity, but after 24 h, 4T1 cells in 0.8 mg Fe/ml concentration showed toxicity.

Two-way ANOVA and LSD test indicated that time of incubation has no significant effect on L929 cell viability ($P$ = 0.80), but the concentration of Fe has significant effect on L929 cell viability ($P$ = 0.037). There is also no significant mutual effect between time and concentration in

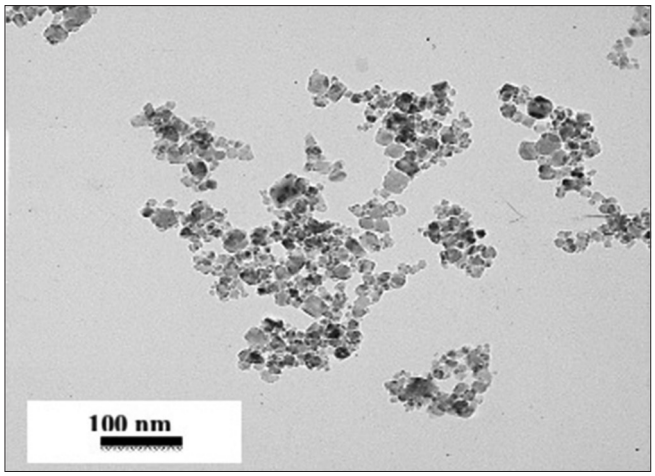


**Figure 1: Transmission electron microscope images of particle size of the polymer-coated nanoparticles**

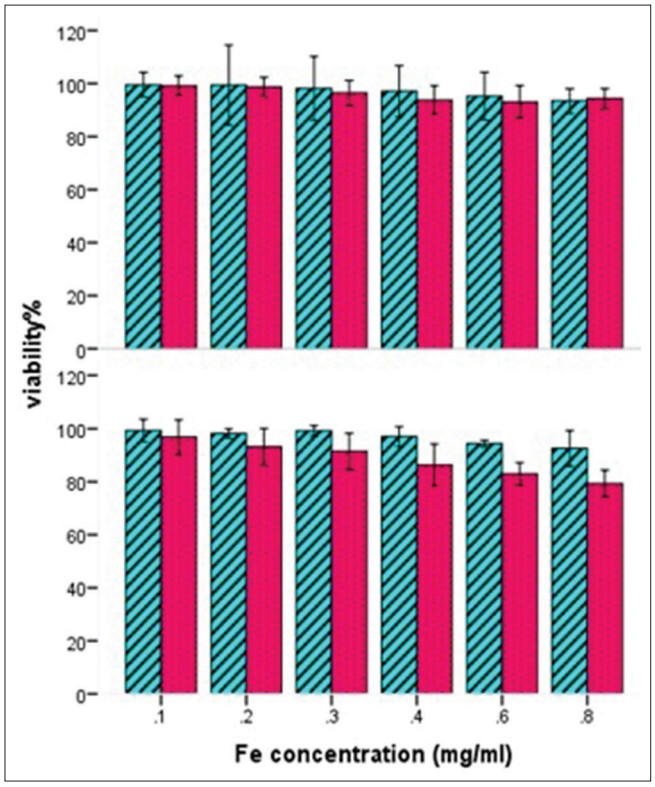


**Figure 3: The viability of 4T1 and L929 cells at time point of (up) 12 h and (down) 24 h after incubation with different concentration of Fe. The value indicates mean ± standard deviation (*n* = 9)**

L929 cell viability ($P = 0.99$) and effect of concentration at L929 cell viability in two times are similar.

The increase of the MNPs concentration up to 0.6 mg Fe/ml causes low toxicity for both studied cells. Hence, the MNPs have no obvious cytotoxicity on these cell lines within the measured concentrations.

### *In vitro* magnetic resonance imaging

Figure 4a indicates $T_2$-weighted MRI of $10^6$ cells from the L929 and 4T1 cells after incubation for 4 h with 0, 0.1, 0.2, 0.4, 0.6, and 0.8 mg Fe/ml of MNPs. Figure 4b is a plot of signal intensity of L929 and 4T1 cells as a function of different Fe concentrations.

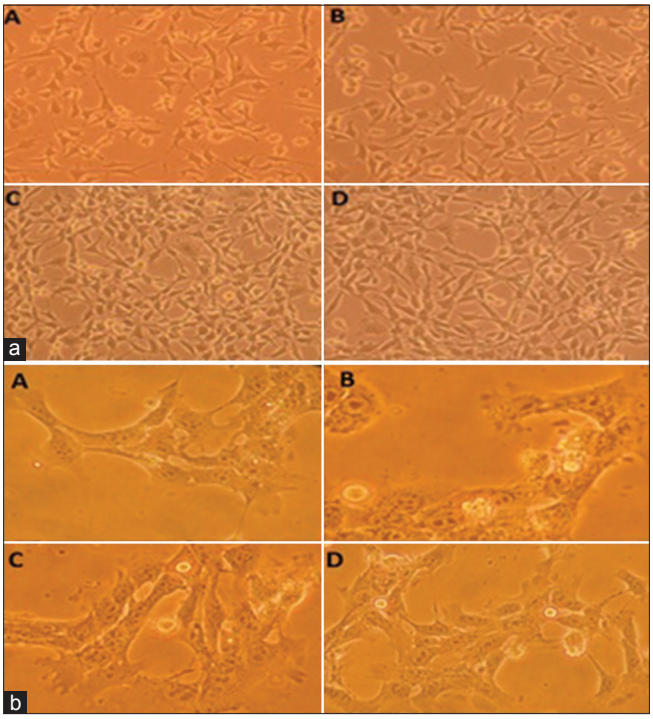


**Figure 2: a) Qualitative cytotoxicity of L929 cells after incubated for 2 h. (A) Without magnetic nanoparticles, (B) with 0.4 mg Fe/ml of magnetic Nanoparticles, (C) the cells were incubated for 24 h without magnetic Nanoparticles, and (D) with 0.4 mg Fe/ml of magnetic nanoparticles. b) qualitative cytotoxicity of 4T1 cells after incubated for 2 h, (A) without magnetic nanoparticles, (B) with 0.4 mg Fe/ml of magnetic nanoparticles, (C) the cells were incubated for 24 h without magnetic nanoparticles, and (D) with 0.4 mg Fe/ml of magnetic nanoparticles**

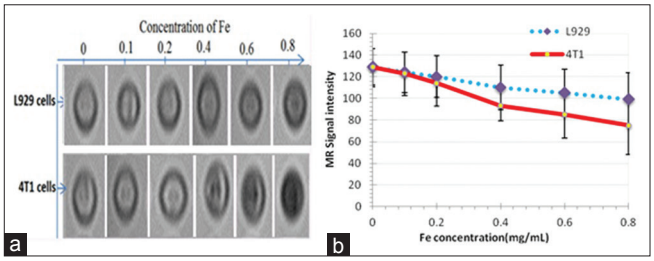


**Figure 4: (a) $T_2$-weighted magnetic resonance images of L929 and 4T1 cells after incubation for 4 h with various concentrations of magnetic nanoparticles. (b) Signal intensity of magnetic resonance images of 4T1 and L929 cells as a function of different incubated concentration of Fe**

Furthermore, Pearson's coefficient correlation test represented that Fe concentration of MNPs has a straight relationship with signal intensity of 4T1 ($P = 0.004$, $r = 0.963$) and L929 ($P = 0.001$, $r = 0.991$) cells.

### Relaxivity ($r_2$) measurements

The potential of MNPs as $T_2$ MRI contrast agent determined by $T_2$-weighted images of different concentrations of MNPs dispersed in water is shown in Figure 5a. The distinctive reduction of signal intensity

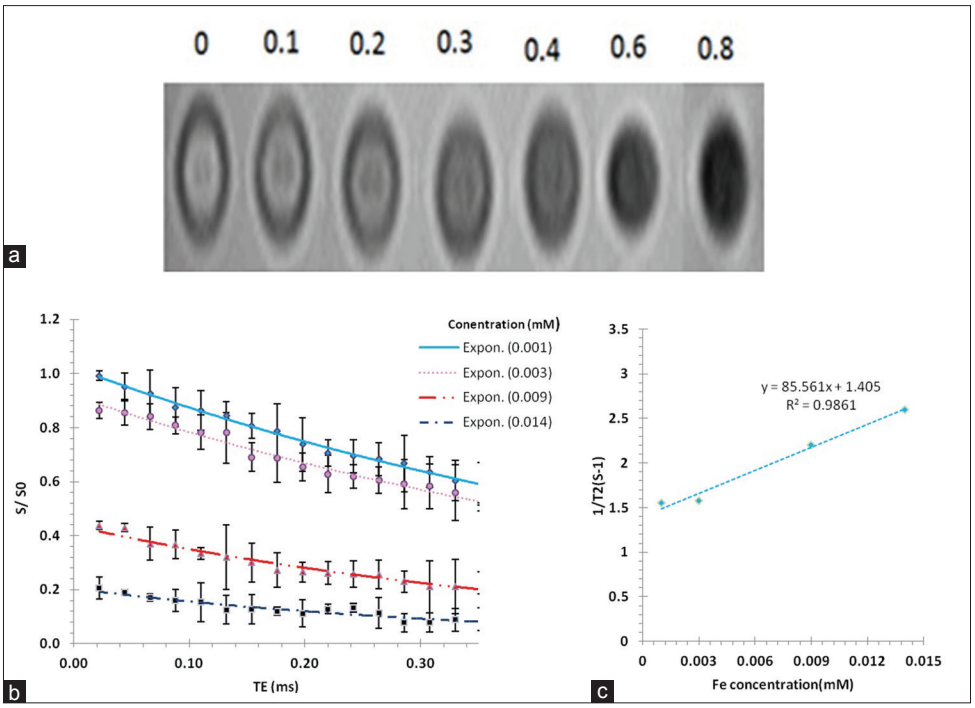


**Figure 5: (a) $T_2$-weighted magnetic resonance images of different Fe concentrations using 1.5 T, standard spin-echo sequence: $T_R$ = 3000 ms, TE = 66 ms. (b) Plots of signal intensity ($S/S_0$) as a function of $T_E$ for different Fe concentration (mM). The signal intensity for each sample was measured three times. (c) Plot of relaxometry rate as a function of Fe concentration (slope of this curve is $r_2$ relaxivity [$mM^{-1}s^{-1}$])**

exists with increasing concentration. The signal intensity in every time echo at various concentrations of Fe (mM) was measured by Image J software. Figure 5b shows the plot of signal intensity ($S/S_0$, S = signal intensity of sample, $S_0$ = signal intensity of control) for MNPs as a function of $T_E$ for different Fe (mM) concentrations, which were drowned in the Excel 2013. Figure 5c shows the $1/T_2$ and relaxivity values of samples. The signal intensity decreases by increasing Fe concentration. Moreover, the value of relaxivity ($r_2$) was obtained 85.5 $mM^{-1}s^{-1}$. These MNPs are classified as negative MRI contrast agent.

## Discussion

In this work, crystalline MZF NPs with core size of 14 nm were successfully obtained by environmental-friendly hydrothermal method and subsequently modified with biocompatible polymer of PEG. To improve their size, monodispersity, crystallinity and activate their surface, the sample was subjected to an acid treatment. Acid-treated MZF NPs were coated with citric acid,[14] providing the carboxylic groups necessary for the formation of an amide group with the amines present on the polymers.

Figure 2a and b shows that cells were spread and they had uniformity shape and division; however, after 24 h, division of 4T1 cells seems lower than control cells and the cells have spherical shape.

Cytotoxicity and relaxometric properties of PEG-coated MZF NPs were investigated as $T_2$ MR imaging contrast agent. An important finding is that MNPs have shown good biocompatibility (the viability of over 80% for 4T1 and L929 cell lines incubated with different Fe concentration at 12 and 24 h in MTT result) and high contrast resolution between normal and cancer cells. The MRI signal intensity of 4T1 cells was lower than that of L929 cells, which indicated MNPs are suitable as $T_2$-weighted MRI contrast agents.

As can be seen from Figure 3, there was a certain degree of decrease in 4T1 cell viability with increasing the concentration ($P < 0.001$) and time ($P < 0.001$). Mutual effect between time and concentration on 4T1 viability is significant ($P = 0.002$) which means the effect of concentration at viability in 24 h were more than 12 h. From the point of statistically view, *t*-test is shown that the viability difference between L929 and 4T1 is significant at 24 h ($P < 0.05$).

Since the purpose of designing MNPs is the ability to use as an MRI contrast agent and detecting cancer cells, the MRI was carried out under *in vitro* conditions. Figure 4a indicates $T_2$-weighted MRI of L929 and 4T1 cells after 4 h incubation. Figure 5b is a plot of signal intensity of L929 and 4T1 cells as a function of different Fe concentrations.

The difference between the image signal intensity of both normal and cancer cells [Figure 5a and b] indicated that the MNPs can be distinguished and differentiated and confirmed ability of the MNPs as MRI contrast agent for studied cells.

MNPs cause drastically darkened $T_2$-weighted MRI of 4T1 cells and brighter for L929. With increasing concentrations of MNPs, the signal intensity and the gray-scale level of the image for both studied cell types

decrease, but the signal intensity and gray-scale level of 4T1 cancer cell images decrease further than normal L929 cell as compared to control group (without MNPs).

The prepared NPs have shown $r_2$ value (85.5 $mM^{-1}s^{-1}$) higher than that reported values for Sinerem (with dextran coated). Higher magnetic moment of these samples due to the substitution of Mn and Zn elements into ferrite structure, in conjunction with the smaller core size and higher polydispersity of Endorem and Resovist, explains the higher relaxivities of studied samples.

Faraji *et al*.,[6] applied PEG polymer as a coating shell on the synthesized NPs and can improve the stability of dispersions containing of the PEG-coated Mn-ferrite NPs at pH = 7, but they did not apply it in any cells under *in vitro* conditions. Also, Fazel Ghaziyani *et al*.,[17] used CD24-PEGylated Au NPs to improve the ability of Computed tomography scanning (CT scan) outputs for both *in vitro* and *in vivo* detection of breast cancer (4T1) cells. In addition, a toxicity research work was performed by Herynek *et al*., on rat mesenchymal stem cells and C6 glioblastoma cells.[18] They have conducted that the studied cells produced a distinct hypointense signal in $T_2$-or $T_2$*-weighted MRI *in vivo*. The results of both mentioned studies and the results of the present work are in a good agreement to confirm the hypothesis of important issues of MZF NPs as an MRI contrast agent for cancer detection.

## Conclusion

Cytotoxicity investigation on the 4T1 and L929 cell lines showed that these NPs led to high cell viability, resulting in good candidates for *in vitro* applications as MRI contrast agents.

For a given MNPs size, the observed $r_2$ relaxivity values are found to be higher than that reported values for commercially clinical used contrast agents such as Sinerem, thereby demonstrating the role of MNPs as a novel $T_2$-weighted MRI. It can be concluded that the hydrothermally synthesized PEG-coated MZF NPs in this study can be a good candidate as MRI contrast agents for the detection of breast cancer cells (4T1).

### Financial support and sponsorship

This work was financially supported by Isfahan University of Medical Science (Grant No: 396146 and 196144).

### Conflicts of interest

There are no conflicts of interest.

## References

1. Shahbazi-Gahrouei D. Novel MR imaging contrast agents for cancer detection. J Res Med Sci 2009;14:141-7.
2. Ghasemian Z, Shahbazi-Gahrouei D, Manouchehri S. Cobalt zinc ferrite nanoparticles as a potential magnetic resonance imaging agent: An *in vitro* study. Avicenna J Med Biotechnol 2015;7:64-8.
3. Shahbazi-Gahrouei D, Moradi Khaniabadi P, Moradi Khaniabadi B, Shahbazi-Gahrouei S. Medical imaging modalities using nanoprobes for cancer diagnosis: A literature review on recent findings. J Res Med Sci 2019. DOI: 10.4103/jrms.JRMS_437_18.
4. Joshi HM. Multifunctional metal ferrite nanoparticles for MR imaging applications. J Nanopart Res 2012;15:1235.
5. Weinreb JC, Abu-Alfa AK. Gadolinium-based contrast agents and nephrogenic systemic fibrosis: Why did it happen and what have we learned? J Magn Reson Imaging 2009;30:1236-9.
6. Faraji S, Dinia G, Zahraei M. Polyethylene glycol-coated manganese-ferrite nanoparticles as contrast agents for magnetic resonance imaging. J Magn Magn Mater 2019;475:137-45.
7. Jadhav SV, Shewale PS, Shin BC, Patil MP, Kim GD, Rokade AA, *et al.* Study of structural and magnetic properties and heat induction of gadolinium-substituted manganese zinc ferrite nanoparticles for *in vitro* magnetic fluid hyperthermia. J Colloid Interface Sci 2019;541:192-203.
8. Keshtkar M, Shahbazi-Gahrouei D, Khoshfetrat SM, Mehrgardi MA, Aghaei M. Aptamer-conjugated magnetic nanoparticles as targeted magnetic resonance imaging contrast agent for breast cancer. J Med Signals Sens 2016;6:243-7.
9. Cabrera LI, Somoza Á, Marco JF, Serna CJ, Morales MP. Synthesis and surface modification of uniform $MFe_2O_4$ (M=Fe, Mn, and Co) nanoparticles with tunable sizes and functionalities. J Nanopart Res 2012;14:873.
10. Zahraei M, Monshi A, del Puerto Morales M, Shahbazi-Gahrouei D, Amirnasr M, Behdadfar B. Hydrothermal synthesis of fine stabilized superparamagnetic nanoparticles of Zn2+substituted manganese ferrite. J Magn Magn Mater 2015;393:429-36.
11. Ruiz A, Salas G, Calero M, Hernández Y, Villanueva A, Herranz F, *et al.* Short-chain PEG molecules strongly bound to magnetic nanoparticle for MRI long circulating agents. Acta Biomater 2013;9:6421-30.
12. Gonzalez-Rodriguez R, Granitzer P, Rumpf K, Coffer JL. New MRI contrast agents based on silicon nanotubes loaded with superparamagnetic iron oxide nanoparticles. R Soc Open Sci 2018;5:180697.
13. Zahraei M, Marciello M, Lazaro-Carrillo A, Villanueva A, Herranz F, Talelli M, *et al.* Versatile theranostics agents designed by coating ferrite nanoparticles with biocompatible polymers. Nanotechnology 2016;27:255702.
14. Cheraghipour E, Javadpour S, Mehdizadeh AR. Citrate capped superparamagnetic iron oxide nanoparticles used for hyperthermia therapy. J Biomed Sci Eng 2012;5:715.
15. Milanovic M, Stijepović I, Pavlovic V, Srdic V. Functionalization of zinc ferrite nanoparticles: Influence of modification procedure on colloidal stability. Process Appl Ceram 2016;10:287-93.
16. Ghahremani F, Shahbazi-Gahrouei D, Kefayat A, Motaghi H, Mehrgardi MA, Javanmard SH. AS1411 aptamer conjugated gold nanoclusters as a targeted radiosensitizer for megavoltage radiation therapy of 4T1 breast cancer cells. RSC Adv 2018;8:4249-58.
17. Fazel-Ghaziyani M, Shahbazi-Gahrouei D, Pourhassan-Moghaddam M, Baradaran B, Ghavami M. Targeted detection of the cancer cells using the anti-CD24 bio modified PEGylated gold nanoparticles: The application of CD24 as a vital cancer biomarker. Nanomed J 2018;5:172-9.
18. Herynek V, Turnovcová K, Gálisová A, Kaman O, Mareková D, Koktan J, *et al.* Manganese-zinc ferrites: Safe and efficient nanolabels for cell imaging and tracking *in vivo*. ChemistryOpen 2019;8:155-65.

## BIOGRAPHIES

**Tayebe Sobhani** received her BSc degree in Radiology Technology in 2015 and her MSc in Medical Physics from Isfahan University of Medical Sciences, Isfahan, Iran in 2019. Her research interests include image processing and imaging modalities.

**Email:** tsobhani94@gmail.com

**Daryoush Shahbazi-Gahrouei** Professor of Medical Physics, BSc in Physics (School of Science, Isfahan University, Iran, 1987), MSc in Medical Physics (Tarbiat Modarres University, Tehran, Iran, 1991), PhD in Medical Physics (University of Western Sydney and St. George Cancer Care Centre, Sydney, Australia, 2000).

**Email:** shahbazi@med.mui.ac.ir

**Mahboubeh Rostami** Assistant Professor at the Department of Medicinal Chemistry, School of Pharmacy and Pharmaceutical Sciences, Isfahan University of Medical Sciences, received her PhD degree in Organic Chemistry from Isfahan University and her BA and MSc degrees from Isfahan University of technology and Sharif University of technology Tehran, respectively. She had two postdoctoral research positions during 2012-2016 by the Medicinal Chemistry department of Isfahan University of Medical Sciences. Furthermore, her professional interests focus on synthesis and functionalization of polymeric drug carriers to apply in cancer drug delivery and design of new small molecules in this area.

**Email:** m.rostami@pharm.mui.ac.ir

**Maryam Zahraei** received her BSc degree in Physics in 2006 and MSc degree in Physics from University of Isfahan, Isfahan, Iran in 2009. She got her PhD degree in Biomaterials in 2015 from Isfahan University of Technology, Isfahan, Iran. Her research interests are focused on application of magnetic nanoparticles in medicine.

**Email:** zahraee_maryam@yahoo.com

**Amin Farzadniya** received his MSc of medical imaging technology with emphasis on MRI (Shahid Beheshti University of Medical Science, Tehran, Iran, 2017), BSc in Radiology Technology (Isfahan University of Medical Sciences, Isfahan, Iran, 2013). He is a cooperator of radiography group of Isfahan University of Medical Science as guest lecturer for MRI technique courses.

**Email:** aminfarzadniya@gmail.com